infrastructures

MDPI

Article

Structural Analysis of Flexible Pavements with HMA Exposed to Short-Term Aging

Taciano Oliveira da Silva [1], Klaus Henrique de Paula Rodrigues [1,*], Heraldo Nunes Pitanga [2], Francisco Aureliano Rocha de Vasconcelos Teixeira [1], Kelbia da Silva Santos [1], Paulo Roberto Borges [3], Gustavo Henrique Nalon [4] and Karine de Oliveira Santos [1]

[1] Department of Civil Engineering, Federal University of Viçosa, Viçosa 36570-900, Brazil; taciano.silva@ufv.br (T.O.d.S.); francisco.teixeira@ufv.br (F.A.R.d.V.T.); kelbia.santos@ufv.br (K.d.S.S.); karine.o.santos@ufv.br (K.d.O.S.)
[2] Department of Transportation and Geotechnics, Federal University of Juiz de Fora, Juiz de Fora 36038-330, Brazil; heraldopitanga@ufjf.br
[3] Department of Engineering, Federal University of Lavras, Lavras 37200-900, Brazil; pauloborges@ufla.br
[4] Department of Applied and Computational Mechanics, Federal University of Juiz de Fora, Juiz de Fora 36038-330, Brazil; gustavo.nalon@ufjf.br
* Correspondence: klaus@ufv.br; Tel.: +55-31-988803578

Abstract

This study presents a comparative evaluation of the structural performance of flexible pavements made from different hot mix asphalt (HMA). HMAs were proportioned using the conventional Marshall method and HMAs subjected to short-term aging were analyzed. Grades B (binder course) and C (surface course), according to DNIT specifications, were used. After determining the aggregate gradation and asphalt content using the Marshall method, test specimens were produced and tested in the laboratory to determine the mechanical parameters characteristic of each HMA (stability, tensile strength by diametral compression, resilient modulus, fatigue behavior, and permanent strain). The Elsym5 software was used to carry out a structural analysis of an assumed pavement, whereby only the mechanical properties of the surface course and the binder course were varied. The results showed that short-term aging significantly affected the mechanical behavior of HMA and the structural response of flexible pavements. Better structural performance was observed in HMAs subjected to short-term aging. The aged specimens showed an improvement in mechanical properties compared to specimens produced by the conventional method, indicating a promising approach for optimizing pavement performance. These results provided new parameters for investigation and development in the field of road engineering.

Keywords: HMA; Marshall method; short-term aging; structural pavement analysis

Check for updates

Academic Editors: Giuseppe Cantisani, Xiao Chen and Guangji Xu

Received: 30 October 2025
Revised: 22 November 2025
Accepted: 6 May 2026
Published: 9 May 2026

Copyright: © 2026 by the authors. Licensee MDPI, Basel, Switzerland. This article is an open access article distributed under the terms and conditions of the Creative Commons Attribution (CC BY) license.

1. Introduction

The aging process of hot mix asphalt (HMA) can be divided into two phases: short-term aging, which is associated with exposure to air and heat during the production of HMA, and long-term aging, which develops throughout the service life of the HMA [1,2]. Given its influence on the rheological properties of asphalt binders, aging has been the subject of studies in recent decades aimed at incorporating control criteria into material specifications [3].

The Marshall method, which is proposed in the technical standard ME 447 [4], does not prescribe short-term aging of the HMA, as this process is a reproduction of the effect

that occurs during the production of an HMA. The Superpave method, on the other hand, takes this requirement into account and prescribes two hours of aging in an oven using the same temperature used for the compaction of the HMA.

For Shah, et al. [5], several factors influence the mechanical behavior of HMA, such as temperature, aggregate type, and volumetric variables. Some factors occur regardless of the type of asphalt and aggregates used, including the aging of the HMA, more specifically the aging of the asphalt binder [2]. Briliak and Remišová [3] add that the most important change in the rheological behavior of materials caused by aging is the increase in stiffness, both during the short-term and in long-term aging. Same observations were made by Pradhan [6] and Albayati and Abduljabbar [1], who attributed the increase in the stiffness of HMA in the field to the additional increase in viscosity due to the effects of aging of the asphalt binder in service.

As discussed in the work of Albayati and Abduljabbar [1], the aging of asphalt binders occurs in two main phases. The first phase, short-term aging, mainly takes place during the production and application of the HMA. This process is intensified by high temperatures and exposure to oxygen, leading to increased stiffness of the asphalt due to the evaporation of volatile components and oxidation. The second phase, long-term aging, as studied by Li, et al. [7], results from constant exposure to environmental conditions such as ultraviolet radiation and temperature fluctuations, which lead to progressive oxidation that increases susceptibility to cracking and pavement failure.

According to Mohammad Asib, et al. [8], given the inevitable aging and associated hardening of the HMA, it is important to investigate and research how the aging process takes place and how the stiffness and resistance of the HMA changes. Zheng, et al. [9] found that after aging, the asphalt binder showed a reduction in the penetration value at 25 °C, reduced ductility, and an increase in the softening point. These characteristics indicate that greater attention must be paid to the temperature limits of HMA, as these properties can affect performance.

Analyzing the aging of asphalt binders in isolation is common practice but is not sufficient to fully understand the effects on the performance of asphalt pavements. According to Albayati and Abduljabbar [1], this approach may neglect the interactions between the asphalt and other components of the HMA, such as aggregates, which are critical for a comprehensive understanding of the behavior of HMA. Liu, et al. [2] emphasized the importance of aggregate morphology and its distribution in the mixture, which, together with binder aging, determines the mechanical strength of the pavement. Li, et al. [7] also emphasized that environmental factors such as temperature and exposure to oxidizing agents play important roles in the rate and properties of asphalt aging.

Shah, et al. [5], while investigating various parameters of HMA dosage such as stiffness, concluded that temperature is a predominant factor in analyzing the behavior of these materials.

Liu, et al. [2] investigated the influence of short-term aging on the asphalt–aggregate system and concluded that the changes resulting from the aging process of the asphalt reduce the adhesion between the asphalt and the aggregate. This leads to a reduction in interface resistance and contributes to the cracking process of the system.

Sun, et al. [10] and Albayati and Abduljabbar [1] found that the aging of HMA can effectively increase resistance to permanent strain due to the higher viscosity and stiffness of the material, thereby reducing its tendency to deform under applied loads. Aging accelerates the transition to stiffer material states, suggesting that permanent strain is of greater importance in the early stages of pavement service life.

According to Liu, et al. [2], the fatigue life of aged and unaged HMA shows significant differences in terms of performance and durability. Unaged mixtures retain their

original asphalt binder properties, such as greater flexibility and the ability to absorb deformation without cracking, which contributes significantly to a longer fatigue life. In contrast, aged mixtures exhibit higher stiffness and lower ductility due to chemical and structural changes caused by the aging process [1]. In addition, Briliak and Remišová [3] point out that long-term aging increases these effects and further reduces the fatigue life of the HMA.

However, other studies have found that short-term aged mixtures exhibit better binder–aggregate interaction, improving the cohesion and strength of the mixture, which is essential for performance in heavy traffic conditions. This suggests that artificial aging could be an effective method for conditioning HMA prior to application to ensure that performance characteristics better match expected service conditions [11,12].

The use of aged HMA in structural analysis requires attention to changes in mechanical properties and durability, which can significantly reduce the fatigue life of mixtures and increase susceptibility to cracking and structural failure, as highlighted by Albayati and Abduljabbar [1]. In addition, the structural analysis must take into account the deterioration of the adhesion between the aggregates and the asphalt binder, which can weaken the structure of the pavement and increase the potential for cracking [13,14].

Li, et al. [7] found that aging under small deformations improved the fatigue performance of the asphalt binder. On the other hand, fatigue life decreased with increasing deformation. da Silva, et al. [12] also evaluated the mechanical behavior of structural layers with aged HMA and concluded that short-term aging of the mixture led to an improvement in mechanical parameters but did not indicate satisfactory structural performance.

Since several changes occur during the aging of the HMA that directly affect the strength and durability of the material, it becomes clear that it is necessary to evaluate not only the short-term effects of aging but also its effects on the structural analysis of the pavement. Therefore, this study aims to provide a more accurate and complete evaluation of the performance of the material throughout its service life.

Given the above considerations, this work aimed to compare the parameters of HMAs with different gradations proportioned according to the conventional Marshall method with the same parameters of similar mixtures, but taking into account short-term aging. To compare the fatigue life of the mixtures analyzed, a structural analysis was performed using Elsym5 software to check the horizontal tensile strains in the lower fiber of the asphalt layer.

2. Materials and Methods

2.1. Materials

2.1.1. Aggregate Characterization

The aggregates used in this study are of gneissic origin and comprised crushed stone size 0, crushed stone size 1, and stone dust sourced from a quarry located in Ervália, Minas Gerais, Brazil. Figure 1 shows the particle size distribution curves of the aggregates used in this study, which were obtained according to NBR 17054 [15].

Tables 1–3 show the results of the characterization of the mineral aggregates used in this work.

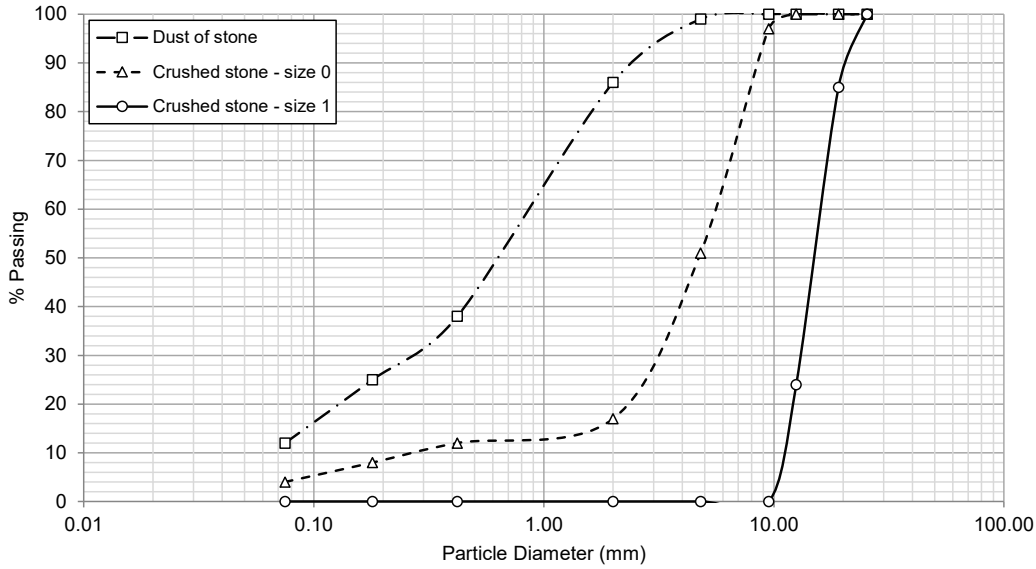

Figure 1. Particle size distribution curves of aggregates.

Table 1. Characterization of the crushed stone (size 1).

Tests	Technical Standards	Results
Percentage of powder material	NBR 16973 [16]	16.66%.
Shape index of coarse aggregates	ME 424 [17]	0.68
Absorption—crushed stone (size 1) Density—crushed stone (size 1) Bulk density—crushed stone (size 1)	NBR 6458 [18]	1.14% 2.794 g/cm^3 2.722 g/cm^3
Los Angeles abrasion of coarse aggregates	NBR 16974 [19]	45%
Adhesion between coarse aggregates and asphalt binder	NBR 12583 [20]	Satisfactory with the addition of 0.1% doping agent

Table 2. Characterization of the crushed stone (size 2).

Tests	Technical Standards	Results
Absorption—crushed stone (size 0) Density—crushed stone (size 0) Bulk density—crushed stone (size 0)	NBR 6458 [18]	1.14% 2.794 g/cm^3 2.722 g/cm^3

Table 3. Characterization of the fine aggregates.

Tests	Technical Standards	Results
Density—fine aggregates	NBR 6458 [20]	2.798 g/cm^3

2.1.2. Characterization of the Asphalt Binder

Asphalt cement 50/70, from the Gabriel Passo refinery (REGAP), located in the municipality of Betim, Minas Gerais, Brazil, was used as the binder. Table 4 shows the results of the characterization tests for the asphalt binder AC 50/70.

The results of the adhesion test between the asphalt binder and the aggregates were not satisfactory. This mismatch was corrected by adding 0.1% of an adhesion-enhancing additive to the binder in relation to the mass of the asphalt cement 50/70.

Table 4. Results of the characterization of the asphalt binder AC 50/70.

Tests	Technical Standards	Results
Penetration	NBR 6576 [21]	56.93 (0.1 mm)
Softening point	NBR 6560 [22]	51 °C
Flash point	NBR 11341 [23]	343 °C
Fire point	NBR 11341 [23]	365 °C
Specific mass	NBR 6296 [24]	1.010 g/cm^3
Relative density	NBR 6296 [24]	1.006 g/cm^3
RTFOT—retained penetration	NBR 6576 [21]	67%
RTFOT—softening point increase	NBR 6560 [22]	3.8 °C
RTFOT—ductility at 25 °C	NBR 6293 [25]	>150 cm
RTFOT—% variation in weight	NBR 15235 [26]	−0.003%
Solubility in trichloroethylene	NBR 14855 [27]	100% mass
Brookfield rotational viscosity 135 °C		318 cP
Brookfield rotational viscosity 155 °C	NBR 15184 [28]	162 cP
Brookfield rotational viscosity 170 °C		51 cP

2.2. Methods

In order to perform the structural analysis based on an ideal pavement configuration, the HMAs were designed using the Marshall proportioning method according to ME 447 [4]. Subsequently, half of the mixtures were subjected to a short-term aging process. The mechanical performance of the mixtures was evaluated through laboratory tests, which included tests of tensile strength by diametrical compression (TS), resilient modulus (RM), fatigue life and permanent strain (static creep).

In the structural analysis used in this work, a constant pavement structure consisting of a base course, sub-base and subgrade reinforcement was maintained for all investigated situations. Variations occurred only in the HMAs used in the asphalt layer, which were divided into surface and binder courses. For the base course, HMAs with DNIT gradation C were analyzed using the conventional method (HMA-C) and with aging. For the base course, HMAs with DNIT gradation B were analyzed using the conventional method (HMA-B) and with aging. Elsym5 software was used to determine the stresses, strains and displacements acting on the analyzed pavement structure.

2.2.1. Marshall Mix Design Method

Two hot mix asphalts (HMA) were selected whose particle size compositions fall into the C and B gradations of ES 031 [29], namely gradation C, which is used as a surface course, and gradation B, which is used as a binder course.

Table 5 contains the limit values for gradation C and B for air voids (AV), voids filled with asphalt (VFA), minimum Marshall stability and minimum TS. Values established by standard ES 031 [29].

Table 5. Limit values for particle size gradations B and C according to ES 031 [29].

Parameters	Gradation B	Gradation C
AV (%)	4.0 to 6.0	3.0 to 5.0
VFA (%)	65–72	75–82
Marshall stability, min (kgf)	500	500
TS, min (MPa)	0.65	0.65

Five experimental values were established for each area studied based on previous experiments with HMA already produced in the laboratory using the same materials. The experimental HMA-C values were 4.0%, 4.5%, 5.0%, 5.5% and 6.0%, and for HMA-B they were 3.5%, 4.0%, 4.5%, 5.0% and 5.5%. Three specimens were prepared for each binder

content to allow further calculations of average values of different parameters. The mixtures were prepared with the binder maintained at a temperature of 159 °C, and the aggregates were heated to 174 °C. These temperatures were selected based on the viscosity–temperature curve of the binder, as recommended by ME 004 [30].

The specimens were compacted using a Marshall compactor with a compaction effort of 75 blows per side, as prescribed by ES 031 [29]. The voids in the mineral aggregate (VMA) were also determined for both mixtures. For the surface course mixture (gradation C), the VMA was 15.41%, whereas for the binder course mixture (gradation B), the VMA was 14.86%.

After obtaining the volumetric and mechanical parameters, Marshall stability and creep values were determined according to ME 447 [4]. The asphalt binder's design content was determined by analyzing the variation in air voids (AV) and voids filled with asphalt (VFA) in terms of the five initial binder contents.

The design values of the asphalt binder for each gradation are listed in Table 6.

Table 6. Design asphalt binder contents for the Marshall mix design method.

Method	Design Asphalt Binder Content (%)	
	Gradation B	Gradation C
Marshall	4.20	4.70

2.2.2. Particle Size Distribution Curves for Marshall Mix Design

Figure 2 shows the design particle size distribution curve corresponding to gradation B according to ES 031 [29].

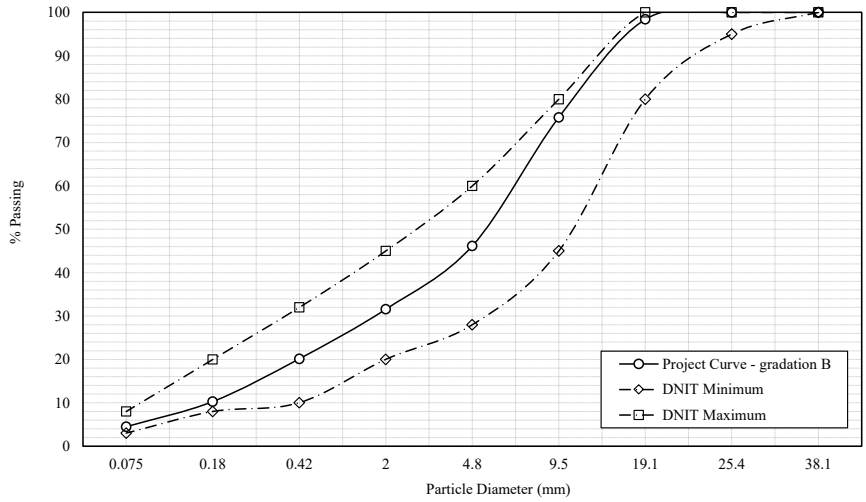

Figure 2. Particle size distribution curve for HMA-B.

Figure 3 shows the design particle size distribution curve that fulfils the gradation C according to ES 031 [29].

Various aggregate contents were tested to determine the granulometric composition of the individual mixtures. The design curve for mixture gradation B was defined as 32% crushed stone 1, 41% crushed stone 0 and 27% stone dust, whereas the design curve for gradation C was defined as 20% crushed stone 1, 46% crushed stone 0 and 34% stone dust. The particle size distribution curves defined for gradations B and C corresponded to the requirements and limit values specified in ES 031 [29].

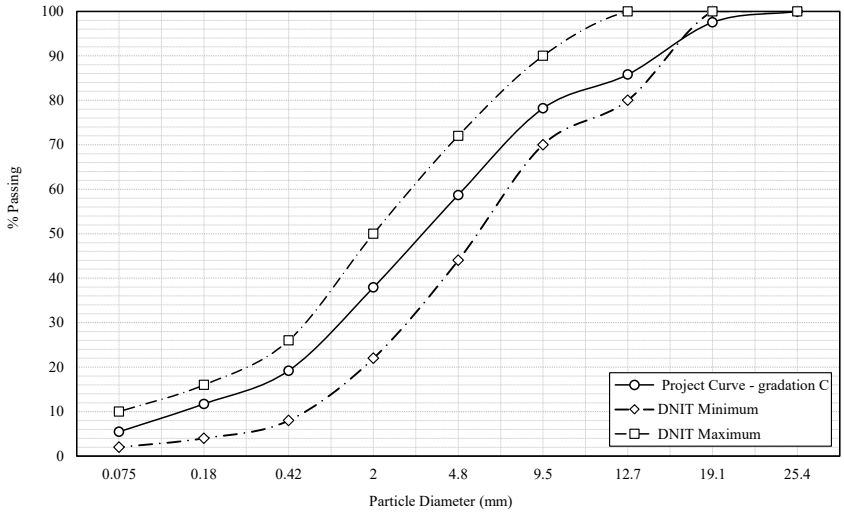

Figure 3. Particle size distribution curve for HMA-C.

2.2.3. Aging Method

After the HMAs had been produced using the Marshall mix design method, part of the mixtures was subjected to a short-term aging process. For this purpose, the mixtures were stored for two hours in an oven at the temperature specified for compaction according to the Superpave mix design method presented by Bernucci, et al. [31].

Short-term aging was used to simulate the period during which the HMA is processed, transported and placed on-site for compaction in order to analyze its influence on the behavior of the mixtures.

2.2.4. Mechanical Tests to Evaluate the Behavior of HMA

The HMA with and without aging were evaluated in terms of mechanical performance through laboratory tests of TS, RM, fatigue life and permanent strain (static creep). In addition, the Shapiro–Wilk test, Levene's test, and t-tests (with Welch's correction when required) were applied to compare aged and non-aged mixtures for TS, Marshall stability, and RM.

Marshall Stability Test

The Marshall stability and flow properties of the mixtures were evaluated in accordance with ME 447 [4]. Cylindrical specimens with a diameter of 100 mm and a height of 63.5 mm were conditioned in a thermostatic water bath at 60 °C for a period ranging from 30 to 40 min. Immediately after conditioning, the specimens were placed in the Marshall loading frame and subjected to monotonic compression at a deformation rate of 50 mm/min. During testing, the applied vertical load and the corresponding deformation were continuously measured, allowing for the determination of the stability and flow parameters.

The mixtures subjected to short-term aging were tested following the same Marshall procedure described above, with the only difference being that they underwent laboratory short-term aging prior to compaction.

Tensile Strength by Diametral Compression

The TS of the mixtures was determined in accordance with ME 136 [32]. Cylindrical specimens with a diameter of 100 mm and a height of 63.5 mm were conditioned for 4 h in an oven at 25 °C to ensure thermal equilibrium prior to testing. The specimens were then positioned in the testing machine with loading strips placed along the vertical diametral plane. A monotonic load was applied at a constant rate of 0.8 mm/s until specimen failure.

The maximum load recorded immediately before rupture was used to calculate the TS according to the classical Brazilian tensile test equation. Each mixture was tested using three replicates.

Resilient Modulus Test

The resilient modulus (RM) of the asphalt mixtures was determined according to standard ME 135 [33]. The tests were performed on Marshall-type cylindrical specimens with dimensions of 100 mm in diameter and 63.5 mm in height. Prior to testing, all specimens were subjected to 4 h of thermal conditioning at 25 °C in a controlled temperature oven. A haversine load pulse was applied at a loading frequency of 1 Hz, consisting of 0.1 s of load application followed by 0.9 s of rest.

Fatigue Life Test

The fatigue performance of the mixtures was evaluated using a fatigue test in controlled-stress mode, following the procedures of ME 183 [34]. The tests were performed at 25 °C, using a sinusoidal loading waveform applied at a frequency of 1 Hz. Each loading cycle consisted of a 0.1 s load application period followed by a 0.9 s rest period, totaling 1 s per cycle.

The specimens were tested under six stress levels, representing 15%, 20%, 25%, 30%, 35%, and 40% of their TS. The specimens were cylindrical, with a diameter of 100 mm and a height of 63.5 mm. All tests were performed in a servo-hydraulic testing machine equipped with LVDTs at the Pavement Laboratory of UFJF, Juiz de Fora, Brazil.

Fatigue life (Nf) was defined as the number of cycles required to cause specimen failure, characterized by complete rupture of the specimen.

The fatigue data were fitted using a logarithmic power-law model:

$$Nf = k * (\Delta\sigma)^n \quad (1)$$

where k and n are regression coefficients obtained from the experimental results, and $\Delta\sigma$ is the stress diference.

Static Creep Test

In the investigation of permanent strain, the uniaxial compression test (static creep) was performed according to the methodology described in Report 465 [35]. Static loading at a stress of 0.1 MPa was applied over a period of 60 min, with a further recovery period of 15 min. The entire test was conducted at a controlled temperature of 40 °C.

From the static creep test, the parameters of the average total deformation during the test (Dt), the creep modulus (Mc), the slope of the deformation curve in the secondary phase of its development (I-curve) and the recovery of the deformation that occurred during the static creep test were determined.

2.2.5. Simulation of the Mechanical Behavior of HMA with the Elsym5 Software

In this work, a pavement structure consisting of a surface course, binder course, base course, sub-base course and subgrade reinforcement was assumed for all investigated situations, with only the HMA being varied. Elsym5 software was used to determine the stresses, strains and displacements acting on the pavement structure.

Three types of loads were tested: 80 kN, 98 kN and 118 kN. The horizontal and vertical stresses acting at the bottom of the surface course and binder course were positioned on the central axis of the wheels (x = 0 mm) and on the equidistant axis of symmetry between the two wheels of the standard semi-axis (x = 162 mm), verifying the most critical situation

between these points for each parameter. The tensile stresses determined for the binder course were also used to evaluate the behavior of the HMA in terms of fatigue life.

For the input data in the Elsym5 software, the RM was assumed to be equal to the modulus of elasticity (E), with linear elastic behavior assumed for the pavement layers. According to Ponte, et al. [36], the Poisson's ratio for the asphalt layers (surface course and binder course) and for the granular layer (base course) must be assumed to be 0.30 if it is not possible to determine it experimentally.

The following load levels were investigated: (i) Q1 equal to 80 kN (8.2 tf), a load equivalent to a standard 18,000 lb axle and the equivalent axle for pavement design in Brazil; (ii) Q2 corresponding to 98 kN (10.0 tf), the maximum load allowed by Brazilian law for single axles with dual wheels; and (iii) Q3 corresponding to 118 kN (12.0 tf), a load that is 20% higher than the maximum allowed load and is used to illustrate the damage caused by overloading of commercial vehicles on the road. In the structural analysis, uppercase Q denotes the total axle load, whereas lowercase q represents the load transmitted by each individual wheel of the axle assembly. Thus, for the dual-wheel configuration adopted in this study, q corresponds to the wheel load associated with each Q loading level. After the three load levels, the following tire inflation pressures were used: (i) P1 equal to 563 kPa (80 psi), which was used to determine deflection according to ME 133 [37]; (ii) P2 equal to 633 kPa (90 psi), which denotes an average pressure level; and (iii) P3 equal to 703 kPa (100 psi), which is a high-pressure level.

Figure 4 illustrates the structure of the assumed pavement and the applied load. The properties of the materials used for the subgrade and subgrade reinforcement were taken from the study by Carmo, et al. [38], whereas the parameters adopted for the base course were taken from the study by Ponte, et al. [36].

In the study by Carmo, et al. [38], the RM of 122.6 MPa corresponds to a subgrade soil classified as LG', A-7-5, CL, compacted under standard Proctor energy and sourced from a soil deposit located between the municipalities of São Carlos and Itirapina (SP). The RM of 401.7 MPa referred to the reinforced subgrade layer produced with a soil classified as A-2-4, SC, LA', also compacted under standard Proctor energy and obtained from a borrow pit in Uberaba (MG). Details regarding soil characterization, specimen preparation and testing conditions are fully described by Carmo, et al. [38].

The laboratory fatigue life results obtained from the fatigue test conducted in accordance with ME 183 [34] were incorporated into the structural fatigue evaluation of the asphalt layers. The fatigue model used in this study relates the stress difference ($\Delta\sigma$) to the number of cycles to failure (Nf), based on the regression equation derived from the laboratory tests.

Elsym5 was then used to compute the vertical and horizontal stresses at the bottom of both the surface and binder courses. The stress difference ($\Delta\sigma$) for each loading position was determined from this stress field. For each evaluated loading position, the $\Delta\sigma$ values calculated by Elsym5 were substituted into the laboratory-derived fatigue equation to estimate the corresponding fatigue life (Nf) of the asphalt layers.

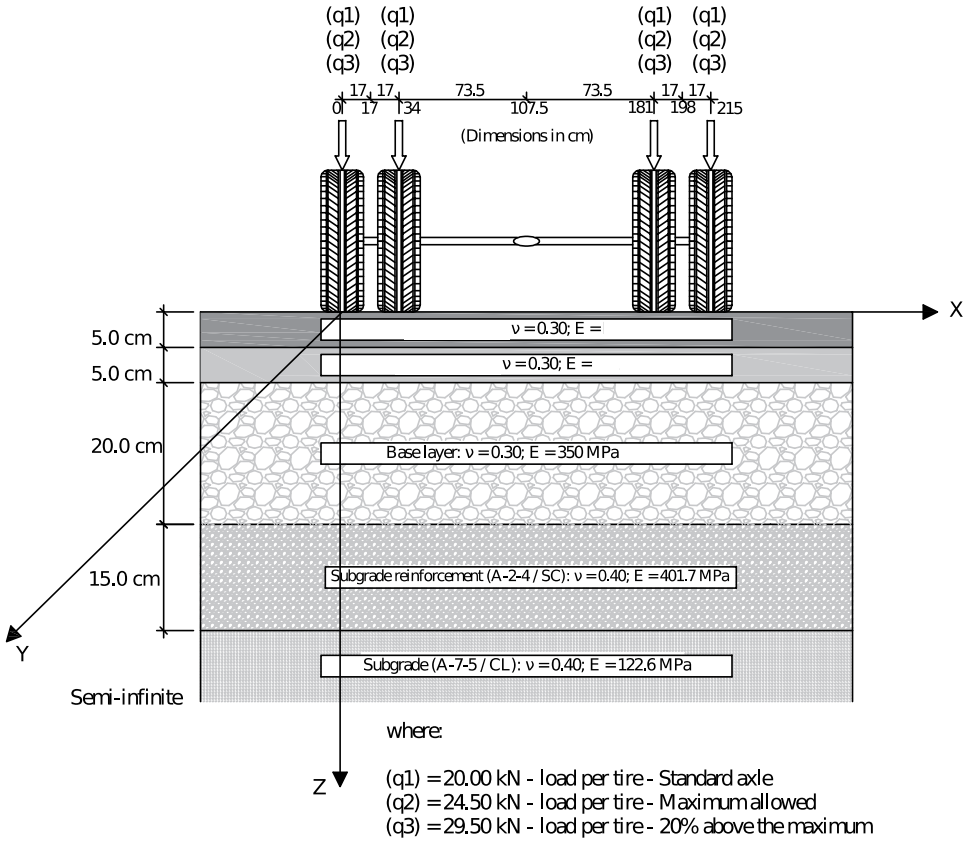

Figure 4. Load patches and loading characteristics. υ—Poisson's ratio.

3. Results

3.1. Mechanical and Volumetric Results

The volumetric properties (air voids (AV) and voids filled with asphalt (VFA)) and mechanical properties (Marshall stability, TS, and RM) were assessed for the surface and binder course mixtures (Table 3). The results for both gradations met the AV and VFA criteria outlined in ES 031 [29]. Additionally, the TS and Marshall stability parameters adhered with the standard specifications. Table 7 shows these results.

Table 7. Mechanical and volumetric results.

Volumetric and Mechanical Parameters	Limits of ES 031 [29]		Design HMA			
	HMA-C	HMA-B	HMA-C (Surface Course)		HMA-B (Binder Course)	
			Non-Aged	Aged	Non-Aged	Aged
Design asphalt binder content (%)	-		4.7	4.7	4.2	4.2
AV (%)	3 to 5	4 to 6	3.7	3.7	4.4	4.4
VFA (%)	75 to 82	65 to 72	75.99	75.99	70.39	70.39
Stability (N)	>4903		5145	8392	5252	7240
Standard deviation			125	479	355	513
TS (MPa)	>0.65		0.91	1.88	0.95	1.43
Standard deviation			0.09	0.08	0.05	0.02
RM (MPa)	-		4073	6659	3948	6443
Standard deviation			137	443	144	267
RM/TS			4476	3542	4156	3806

Figures 5–7 illustrate the Marshall stability, TS, and RM obtained for the aged and non-aged mixtures with gradations C and B, highlighting the influence of short-term aging on

the mechanical behavior of the HMAs. Statistical analysis confirmed that the increases observed in the aged mixtures were significant, as discussed in Section 4.

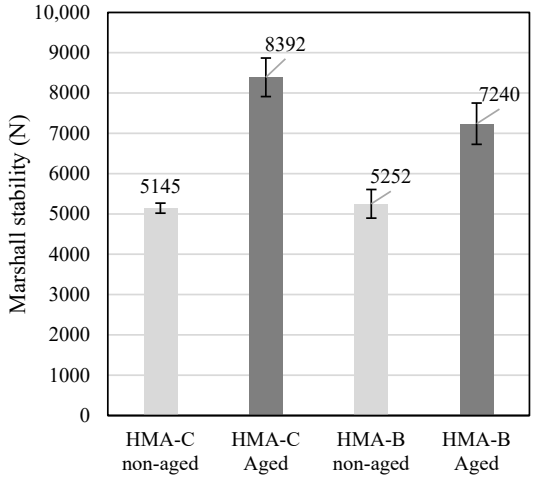

Figure 5. Marshall stability results.

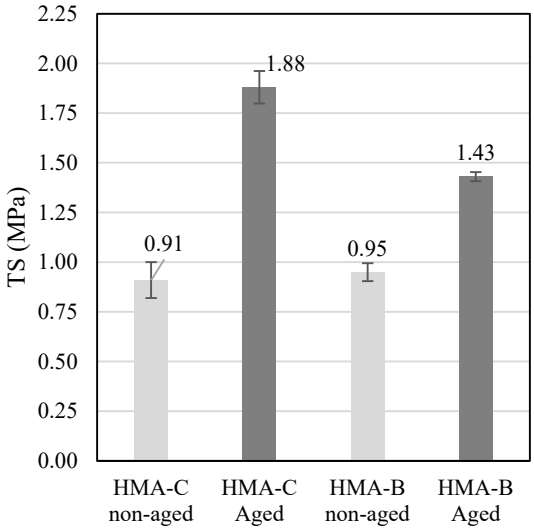

Figure 6. TS results.

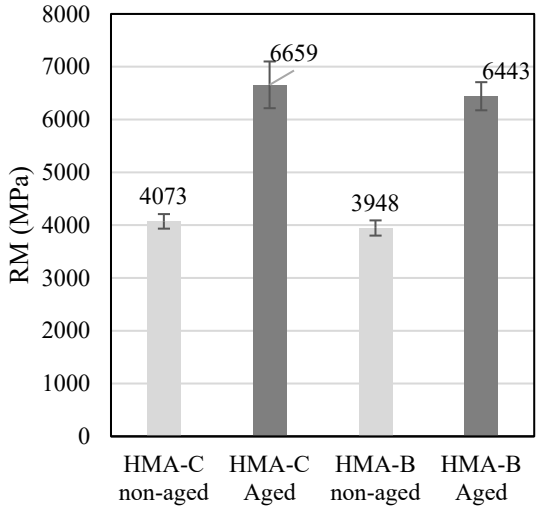

Figure 7. RM results.

3.2. Fatigue Life

Figures 8 and 9 show the results of the fatigue test for HMA-C and HMA-B with and without the aging process, using the Marshall method in accordance with ME 447 [4].

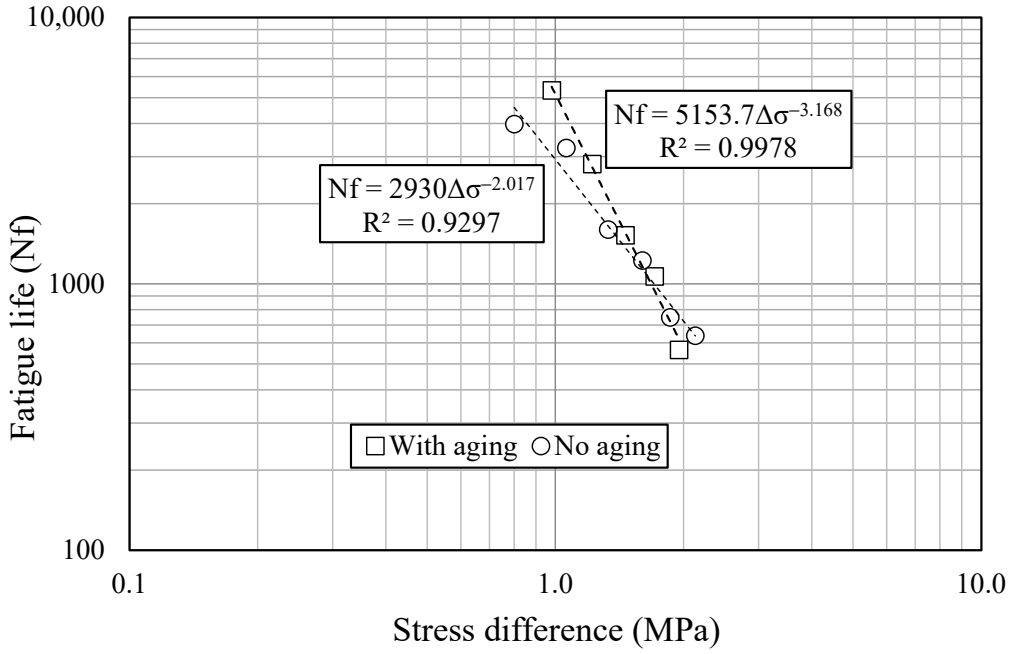

Figure 8. Fatigue life (Nf) versus stress difference (Δσ)—HMA-B.

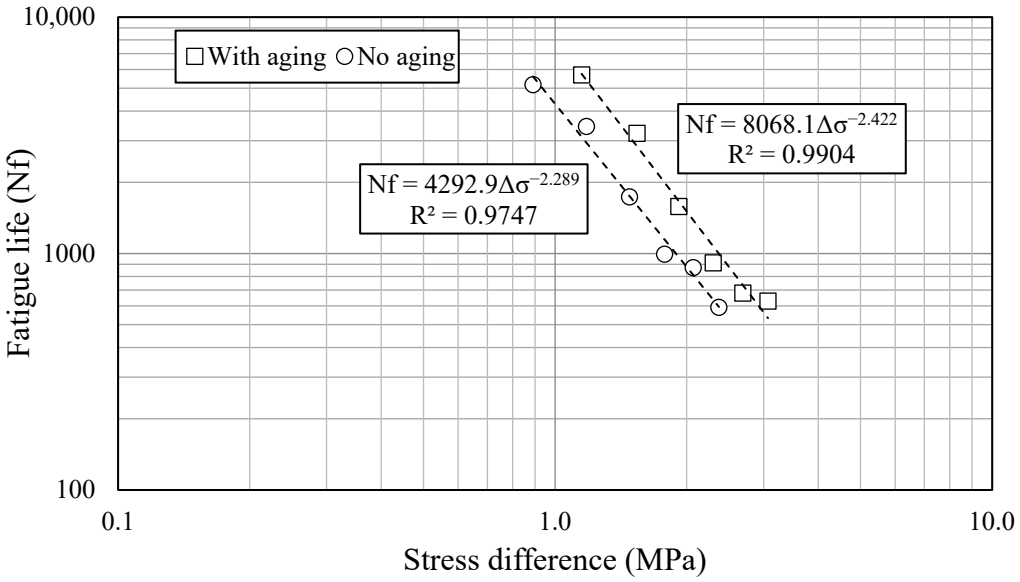

Figure 9. Fatigue life (Nf) versus stress difference (Δσ)—HMA-C.

3.3. Uniaxial Static Compression Creep Test (Static Creep)

Another important parameter that must be taken into account when specifying an asphalt mix for HMA is permanent strain. Table 8 shows the results of the static creep tests on HMA-C and HMA-B with and without the aging process.

Table 8. Average static creep results of mixtures dosed and compacted according to the Marshall method—gradations B and C.

Parameters	HMA-B		HMA-C	
	Conventional	Short-Term Aging	Conventional	Short-Term Aging
Final time (s)	4500	4500	4500	4500
Dt—Total deformation (mm/mm)	0.0059	0.0020	0.0045	0.0007
Mc—Creep modulus (MPa)	19.88	50.55	25.34	175.96
I-curve—Curve slope	0.012	0.017	0.025	0.059
Maximum displacement (mm)	0.44233	0.06832	0.34433	0.17567
Final displacement (mm)	0.38167	0.04799	0.29233	0.13233
Recoverable displacement (mm)	0.0607	0.0203	0.0520	0.0433
Elastic recovery (%)	13.72	42.30	15.10	24.65

3.4. Fatigue Life Analysis of Flexible Pavements

Tables 9–11 show the results of the vertical and horizontal stresses determined for the pavement used in this work at different points of the structure using Elsym5 software. Figures 10 and 11 show the differences in stresses graphically. It was found that the surface course has horizontal and vertical compressive stresses, while the binder course is stressed by tensile stresses, which allows analysis of the behavior of the HMA in this layer in relation to its fatigue life. The horizontal tensile stresses reach their highest value at Z equal to 9.99 cm, in the lower fiber of the binder course. At this depth, the most requested points correspond to positions X equal to 0 cm, and the tensile stresses have positive values and the compressive stresses negative values according to the sign system used by the Elsym5 software.

Table 9. Horizontal (σh) and vertical (σv) stresses acting on the surface course and the binder layer (Q1 = 8.2 t).

Position (cm)			Stresses (kgf/cm^2)					
X	Y	Z	q1 = 2.05 tf					
Surface layer			HMA			Aged HMA		
			σh	σv	|Δσ|	σh	σv	|Δσ|
0.00	0.00	4.99	−1.80	−4.00	2.20	−1.70	−3.80	2.10
8.50			−1.50	−3.30	1.80	−1.40	−3.10	1.70
17.00			−1.20	−0.60	0.60	−1.10	−0.50	0.60
25.50			−1.50	−3.30	1.80	−1.40	−3.10	1.70
34.00			−1.80	−4.00	2.20	−1.70	−3.80	2.10
Binder course			HMA			Aged HMA		
			σh	σv	|Δσ|	σh	σv	|Δσ|
0.00	5.00	9.99	7.90	−1.90	9.80	10.80	−1.50	12.30
8.50			6.90	−1.60	8.50	9.70	−1.40	11.10
17.00			5.10	−1.30	6.40	7.80	−1.10	8.90
25.50			6.90	−1.60	8.50	9.70	−1.40	11.10
34.00			7.90	−1.90	9.80	10.80	−1.50	12.30

Table 10. Horizontal (σh) and vertical (σv) stresses acting on the surface course and the binder layer (Q2 = 10 t).

Position (cm)			Stresses (kgf/cm^2)					
X	Y	Z	q2 = 2.5 tf					
Surface layer			HMA			Aged HMA		
			σh	σv	|Δσ|	σh	σv	|Δσ|
0.00			−2.20	−4.60	2.40	−2.00	−4.30	2.30
8.50			−1.90	−3.90	2.00	−1.80	−3.70	1.90
17.00	0.00	4.99	−1.40	−0.70	0.70	−1.30	−0.70	0.60
25.50			−1.90	−3.90	2.00	−1.80	−3.70	1.90
34.00			−2.20	−4.60	2.40	−2.00	−2.00	2.30
Binder course			HMA			Aged HMA		
			σh	σv	|Δσ|	σh	σv	|Δσ|
0.00			9.30	−2.30	11.60	12.70	−1.80	14.50
8.50			8.20	−1.90	10.10	11.70	−1.70	13.40
17.00	5.00	9.99	6.30	−1.50	7.80	9.50	−1.40	10.90
25.50			8.20	−1.90	10.10	11.70	−1.70	13.40
34.00			9.30	−2.30	11.60	12.70	−1.80	14.50

Table 11. Horizontal (σh) and vertical (σv) stresses acting on the surface course and the binder layer (Q3 = 12 t).

Position (cm)			Stresses (kgf/cm^2)					
X	Y	Z	q3 = 3.0 tf					
Surface layer			HMA			Aged HMA		
			σh	σv	|Δσ|	σh	σv	|Δσ|
0.00			−2.60	−5.10	2.50	−2.40	−4.90	2.50
8.50			−2.30	−4.50	2.20	−2.20	−4.40	2.20
17.00	0.00	4.99	−1.70	−0.90	0.80	−1.60	−0.80	0.80
25.50			−2.30	−4.50	2.20	−2.20	−4.40	2.20
34.00			−2.60	−5.10	2.50	−2.40	−4.90	2.50
Binder course			HMA			Aged HMA		
			σh	σv	|Δσ|	σh	σv	|Δσ|
0.00			10.60	−2.60	13.20	14.70	−2.20	16.90
8.50			9.60	−2.30	11.90	13.70	−2.00	15.70
17.00	5.00	9.99	7.50	−1.80	9.30	11.40	−1.70	13.10
25.50			9.60	−2.30	11.90	13.70	−2.00	15.70
34.00			10.60	−2.60	13.20	14.70	−2.20	16.90

Figure 12 shows the behavior of the binder course in terms of fatigue life (Nf) at different positions along the X-axis.

The pavement section incorporating aged HMA-B and HMA-C in the asphalt layers and subjected to the Q2 load of 98 kN exhibited a higher fatigue life than the pavement designed with the conventional Marshall mixture and loaded with Q1 = 80 kN. It was also observed that the lowest fatigue lives occurred at positions X = 0 cm and X = 34 cm, which correspond to the wheel centerlines, while higher Nf values were obtained at the other transverse positions. The laboratory fatigue lives (Nf,lab) were then calculated for the points subjected to the highest loading, i.e., the number of load repetitions to failure associated with a given stress difference (Δσ), using the fatigue equations established in the laboratory tests (Table 12).

Table 12. Fatigue life—Nf,lab.

Layer	Method	Fatigue Life Equation	Nf,lab		
			q1 = 2.05 tf	q2 = 2.5 tf	q3 = 3.0 tf
Binder course (4.99 a 9.99 cm)	HMA	$2930\|\Delta\sigma\|^{-2.07}$	3174	2280	1704
Binder course (4.99 a 9.99 cm)	Aged HMA	$17{,}837\|\Delta\sigma\|^{-4.422}$	7646	3704	1925

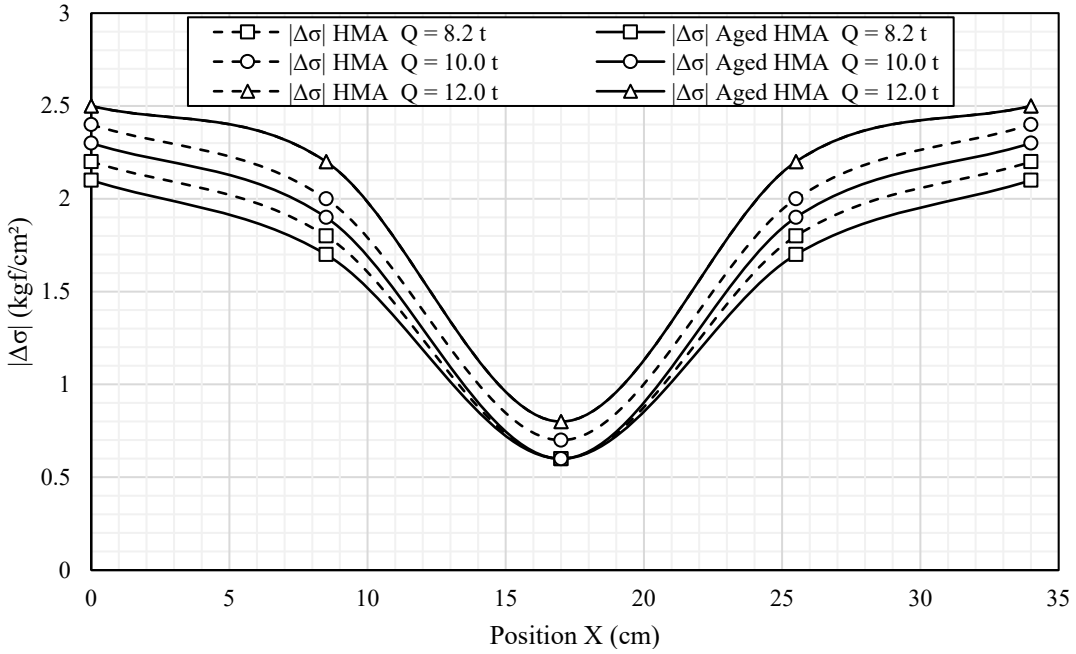

Figure 10. Stress difference (Δσ) acting on the surface course.

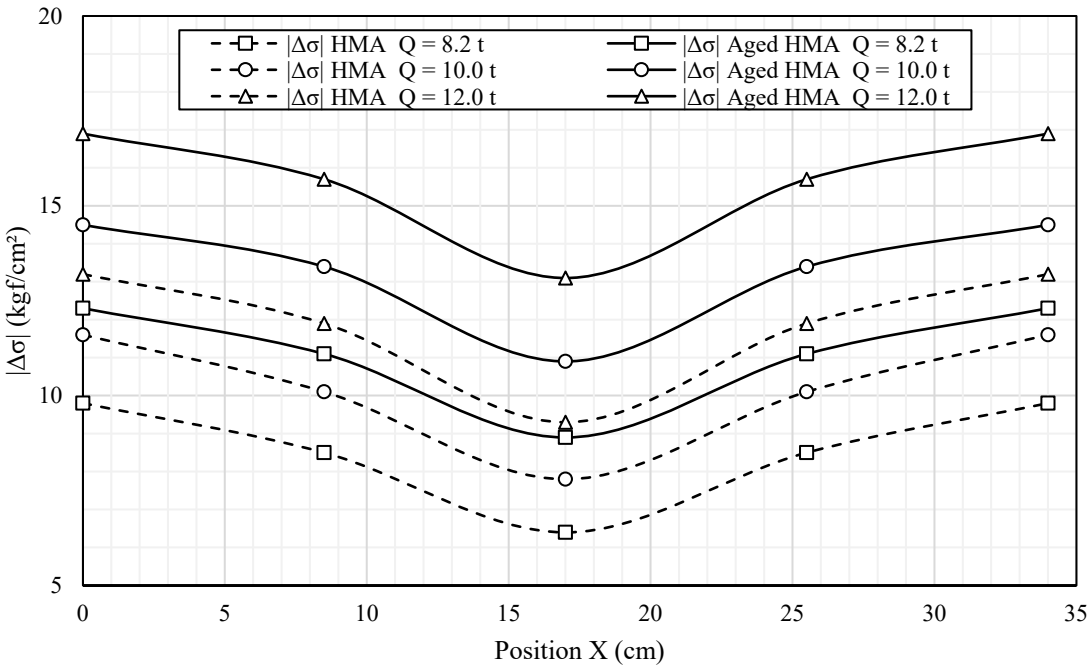

Figure 11. Stress difference (Δσ) acting on the binder course.

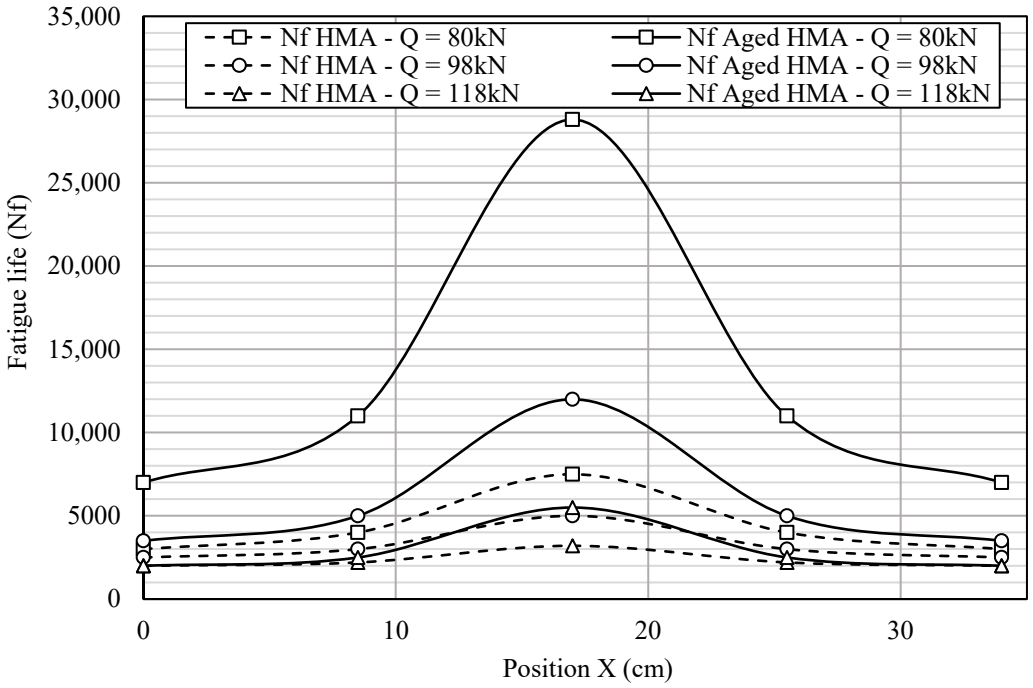

Figure 12. Fatigue life (Nf) at different positions along the X-axis.

For the critical points of the binder course, it was found that the ratio between the fatigue lives of HMA with short-term aging and conventional HMA (NfAged/NfNonaged) is always greater than one, as shown in Table 13. This shows the best structural performance of the binder course obtained with short-term aging of HMA, but with values gradually approaching unity as the axle load Q increases, due to changes in material properties.

Table 13. Relationship between the fatigue lives of aged and non-aged HMAs.

X	Y	Z	$Nf_{Aged}/Nf_{Nonaged}$ Q1 = 80 kN	$Nf_{Aged}/Nf_{Nonaged}$ Q2 = 98 kN	$Nf_{Aged}/Nf_{Nonaged}$ Q3 = 118 kN
0	0	9.99	2.3	1.6	1.1
34			2.3	1.6	1.1

Table 14 shows the values obtained for the deflection at the point on the road surface along the axis of symmetry between the two wheels for the assumed loads (Q1, Q2 and Q3), as well as the allowable deflection corresponding to the traffic volumes N.

Table 14. Recoverable vertical deflections at the top of the assumed pavement: comparison with D_{allow} determined for the standard load.

Position (cm)			N	D_{allow} (x 0.01 mm) PRO 011/79	HMA (Deflection x 0.01 mm)			Aged HMA (Deflection x 0.01 mm)		
X	Y	Z			Q1 = 80 kN	Q2 = 98 kN	Q3 = 118 kN	Q1 = 80 kN	Q2 = 98 kN	Q3 = 118 kN
17	0	0	10^7	59.98	34.88	42.51	50.98	33.34	40.63	48.72
			5×10^7	45.18						

4. Discussion

Overall, short-term aging consistently improved the mechanical response of both HMA-B and HMA-C, with higher stability, tensile strength, resilient modulus, fatigue life, and better resistance to permanent deformation. In this section, these results are inter-

preted in light of the literature, and their implications for pavement structural performance are discussed.

4.1. Mechanical and Volumetric Results

In the specimens subjected to short-term aging, increases in the results of TS, Marshall stability and RM were observed for both HMA-C and HMA-B.

The statistical analysis of TS, Marshall stability, and RM confirmed that short-term aging produced significant improvements in the mechanical behavior of both mixtures. For TS, aged mixtures showed higher values than non-aged mixtures, with p-values below 0.0001 for both HMA-B and HMA-C, indicating a very strong effect of aging on TS. Marshall stability also increased significantly after aging, with $p = 0.039$ for HMA-B and $p = 0.009$ for HMA-C.

Similarly, RM increased substantially with aging. For HMA-B and HMA-C, the differences between non-aged and aged mixtures were statistically significant ($p < 0.0001$ and $p = 0.003$, respectively), reflecting the stiffening of the mixtures due to oxidative hardening of the binder.

In terms of Marshall stability, all HMA mixtures met the minimum value of 5000 N specified in ES 031 [29]. Short-term aging led to a marked gain in performance, with stability increases of approximately 63% for HMA-C and 38% for HMA-B. A similar trend was observed for TS, where aged mixtures showed superior performance, with increases of about 102% for HMA-C and 51% for HMA-B. These improvements in stability, TS, and RM can be attributed to the gain in stiffness caused by volatilization and oxidation of binder components during the short-term aging process [12,39,40].

Regarding the RM results, all values obtained fall within the typical range for HMA at 25 °C. Bernucci, et al. [31] reported that resilient modulus values between 2000 and 8000 MPa are commonly observed for asphalt mixtures at this temperature, which is consistent with the behavior found in this study. Furthermore, da Silva, et al. [12] indicated that processing, storage, and transportation tend to increase RM due to binder oxidation, supporting the trend observed for the aged mixtures.

The RM/TS ratio decreased after the application of the binder aging process. According to Santos, et al. [41], the ratio between RM and TS is an indicator of fatigue performance that combines information on stiffness and mechanical resistance, with lower RM/TS values indicating better HMA behavior. Lower stiffness is desirable to avoid excessive stress concentrations that can lead to premature cracking in asphalt layers, while higher TS improves the mixture's ability to resist tensile forces. Thus, the reduction in RM/TS observed for the aged mixtures suggests a more favorable balance between stiffness and tensile resistance in terms of fatigue life.

4.2. Fatigue Life

The fatigue life results showed a consistent improvement in performance for the short-term aged mixtures compared with the non-aged mixtures for both gradations, HMA-B and HMA-C. Over the entire range of stress differences ($\Delta\sigma$) considered, the aged mixtures systematically exhibited higher fatigue lives for the same $\Delta\sigma$, indicating that they were less susceptible to crack initiation and propagation under repeated loading. In addition, the regression analysis revealed steeper fatigue curves for the aged mixtures, meaning that their fatigue life became more sensitive to changes in stress difference, although at a higher overall performance level than the non-aged mixtures.

This behavior is coherent with the mechanical characterization, which showed simultaneous increases in TS and RM after short-term aging. From a mechanistic point of view, the improved fatigue performance can be interpreted in terms of the balance between stiff-

ness and TS, often expressed by the RM/TS ratio. As discussed by Campelo, et al. [42], RM/TS values on the order of 3000 are associated with favorable structural behavior in fatigue because they represent mixtures that are stiff enough to control tensile strains without becoming excessively brittle. In this study, the aged HMA-B and HMA-C mixtures reached RM/TS levels compatible with this range, which helps explain the superior fatigue lives observed in the laboratory and is consistent with the structural response discussed in the following sections.

4.3. Uniaxial Static Compression Creep Test (Static Creep)

Based on the total deformation (Dt) results, it was found that HMA-C and HMA-B submitted to the aging process had lower susceptibility to permanent strain, which can be explained by the increase in stiffness of the material, as presented by Babadopulos, et al. [43].

For the creep modulus (Mc), Little, et al. [44] indicated a minimum limit of 31.0 MPa for a stress level of 0.1 MPa under conditions of high traffic volume. In the present study, this requirement was only met by the aged HMA-C and HMA-B mixtures, reinforcing the positive effect of short-term aging on resistance to permanent deformation.

Higher slopes (I-curve) are associated with greater susceptibility to permanent strain [45]. In this regard, all tested mixtures complied with the limits recommended by Little, et al. [44] for high-intensity traffic. Although some aged mixtures exhibited slightly higher slopes than the non-aged mixtures, their overall performance, considering Dt, Mc, and the allowable limits, was still better, indicating improved resistance to permanent deformation under static loading.

The superior performance of the aged mixtures in terms of stiffness, fatigue resistance, and resistance to permanent deformation is attributed to significant changes in the properties of the asphalt binder and in the binder–aggregate interaction. Artificially induced short-term aging, as observed by Briliak and Remišová [3], increases the stiffness of the asphalt binder. This increase in stiffness has a positive effect on the ability of HMA to withstand heavy loads without excessive deformation, which is crucial for the durability of the pavement.

In addition, Liu, et al. [2] emphasized that aging can improve adhesion between the asphalt binder and aggregates, resulting in a more cohesive and resistant mixture. This improved adhesion contributes to better resistance to cracking and fatigue, especially under heavy traffic and variable climatic conditions, while also favoring a more uniform stress distribution within the asphalt layer, thereby reducing crack propagation and extending pavement service life.

The results for recoverable deformation also indicate that mixtures subjected to short-term aging exhibit better recovery capacity after load removal, which is consistent with the observed improvements in permanent deformation parameters. Overall, the data obtained from the static uniaxial compression creep test show that HMA-B and HMA-C proportioned according to the Marshall method meet the performance criteria for permanent deformation only when short-term aging of the binder is considered.

4.4. Fatigue Life Analysis of Flexible Pavements

A clear inverse relationship was observed between the applied load level and the predicted fatigue life of the HMA: lower loads resulted in longer fatigue lives and, consequently, a greater number of allowable load repetitions. In addition, mixtures subjected to short-term aging consistently exhibited superior fatigue performance compared with non-aged mixtures. This behavior is consistent with the higher TS and RM values obtained for the aged mixtures, indicating a more favorable balance between stiffness and tensile

resistance. A similar trend was reported by da Silva, et al. [12], while Bernucci, et al. [31] emphasized that mixtures with higher resilient modulus are better able to sustain traffic-induced stresses within the pavement structure, which helps explain the improved fatigue life observed in the present study.

With increasing load, the deformations produced tend to be greater. Ziari, et al. [45] reported that aging increases fatigue life under small deformations; however, fatigue response decreases with increasing degrees of deformation.

According to Liu, et al. [2], aging improves adhesion between the asphalt binder and aggregates, resulting in a more cohesive and crack-resistant mixture, especially under conditions of heavy traffic and climatic variation. Briliak and Remišová [3] also emphasized that short-term aging increases the stiffness of the asphalt binder and thus improves the pavement's resistance to additional loads. This increased stiffness and strength allow aged HMA to perform better on critical parameters for permanent strain and fatigue life, leading to longer maintenance intervals and pavement durability, which in turn results in long-term cost savings and less traffic disruption.

The vertical displacement at the top of the surface course determined with Elsym5 can be compared with the allowable recoverable deflection (Dallow) defined according to PRO 011 [46], taking into account the traffic volume described in the Brazilian pavement manual [29]. As these volumes were determined in relation to the thickness of the surface course, a thickness of 10 cm was used in this work (5 cm for the surface course and 5 cm for the binder course), which corresponds to the following values $10^7 < N < 5 \times 10^7$, where N represents the number of standard axle loads and the load exerted on the road surface corresponds to the standard axle load (Q1 = 80 kN). Although the allowable deflection was calculated for the standard load, the maximum recoverable vertical deflections determined with the computer program Elsym5 for the higher loads (Q2 = 98 kN and Q3 = 118 kN) were also quantified for comparison with this limit reference.

With N of 5×10^7, only the loads of 80 kN and 98 kN met the criterion of allowable deflection. At N equal to 10^7, the deflection achieved was less than the allowable deflection for all loads tested in this work.

The results emphasize the need to control axle loads to avoid exposing pavements to greater than the allowable deflections and, thus, greater susceptibility to fatigue mechanisms. It was also found that the deflections of aged HMAs were lower than the deflections of HMAs without aging. This emphasizes the importance of adding short-term aging into the proportioning Marshall method, leading to the development of structural products that are less susceptible to structural distresses resulting from this deformation mechanism. This is because, as ref. [31] found, deflection is responsible for the majority of cracks during the service life of the pavement and can lead to fatigue.

Short-term aging causes oxidation and the volatilization of light components (saturates and aromatics), leading to chemical transformations where these components are converted into heavier, more polar asphaltenes. This fundamental chemical shift directly affects the test results by increasing material stiffness and viscosity while decreasing penetration and ductility [47–49].

Briliak and Remišová [3] stated that aging increases the stiffness of the asphalt binder and thus improves the ability of HMA to withstand heavy loads without deforming excessively. Secondly, Liu, et al. [2] emphasize that it improves the adhesion between the asphalt binder and the aggregates, making the mixture more cohesive and resistant to cracking, especially under heavy traffic and climatic variations. In addition, Briliak and Remišová [3] reported that it reduces permanent strain and limits plastic deformation over time. By promoting a more uniform distribution of stresses within the asphalt layer, aging also helps to reduce crack propagation and extend pavement service life.

The deflection results obtained from the pavement structural analysis are consistent with the trends observed in the static creep test. In both gradations B and C, mixtures subjected to short-term aging showed better performance than non-aged mixtures, exhibiting lower deflections and improved resistance to permanent deformation under loading.

5. Conclusions

The objective of this study was to compare an HMA proportioned according to the Marshall method prescribed in ME 447 [4] with a similar HMA subjected to short-term aging. It was found that the aged HMA performed better for all parameters studied here for both the B and C gradations of the DNIT, due to the increased stiffness of the asphalt binder and the better absorption of this material by the aggregates. As noted in the literature consulted, short-term aging brings the HMA closer to its application due to the time interval between mixing the materials and compaction in the field.

Short-term aging led to marked improvements in the mechanical properties of both mixtures. For HMA-C, Marshall stability increased from 5150 N to 8397 N, tensile strength increased from 0.91 MPa to 1.88 MPa, and resilient modulus increased from 4073 MPa to 6659 MPa. For HMA-B, stability increased from 5248 N to 7240 N, TS increased from 0.95 MPa to 1.43 MPa, and RM increased from 3948 MPa to 5443 MPa. These numerical gains reinforce the beneficial effect of short-term aging on mixture stiffness and strength and highlight its relevance to the early-life mechanical response of asphalt pavements.

Increases in performance were observed in fatigue and permanent strain tests (static creep), which were the focus of this analysis, as these parameters are directly related to the performance of HMA in road pavements. These two parameters are the most important criteria for the evaluation and acceptance of asphalt pavements because they influence the durability and utility of the pavement, as they are directly related to fatigue cracking and rutting.

When checking the performance of the pavement structure assumed after applying the three load levels in the Elsym5 program, it was found that the Nf,lab values for aged HMA reached higher values than the Nf,lab of HMA without aging in all cases analyzed. However, it was found that the difference between these values became smaller as the load increased. As for the deflections determined in the evaluation of the Elsym5 software, the values for the all HMAs showed similar performance to that which occurred in the static creep test.

The results of the tests carried out therefore indicate that short-term aging improves the performance of the HMA studied, both from the point of view of the laboratory tests and from the structural analysis carried out with the Elsym5 software.

Although this study improves the understanding of the effects of short-term aging on HMA performance, some limitations remain. The experimental program was restricted to a single asphalt binder (50/70), aggregates from one gneissic source, and laboratory-simulated short-term aging, while the structural analysis relied on a linear elastic model. Future studies should investigate the long-term aging of binders and mixtures, including accelerated conditioning with cycles of heat, UV radiation, and moisture; evaluate different binders and modifiers; assess the use of rejuvenators; incorporate nonlinear and viscoelastic numerical models; and validate laboratory findings through field monitoring.

Author Contributions: Conceptualization, H.N.P., T.O.d.S., K.H.d.P.R., and P.R.B.; methodology, P.R.B., T.O.d.S. and H.N.P.; validation, K.H.d.P.R., G.H.N., H.N.P., T.O.d.S., K.d.S.S., F.A.R.d.V.T. and K.d.O.S.; formal analysis, P.R.B., H.N.P., G.H.N. and K.H.d.P.R.; investigation, P.R.B.; resources, T.O.d.S., P.R.B. and H.N.P.; data curation, T.O.d.S., K.H.d.P.R., F.A.R.d.V.T., K.d.S.S. and G.H.N.; writing—original draft preparation, P.R.B. and T.O.d.S.; writing—review and editing, H.N.P., T.O.d.S., G.H.N., K.H.d.P.R., K.d.O.S. and F.A.R.d.V.T.; visualization, H.N.P., G.H.N. and

K.H.d.P.R.; supervision, H.N.P. and T.O.d.S.; project administration, T.O.d.S. All authors have read and agreed to the published version of the manuscript.

Funding: This research received no external funding.

Data Availability Statement: Data are contained within the article.

Acknowledgments: This work was financed in part by the Coordenação de Aperfeiçoamento de Pessoal de Nível Superior—Brasil (CAPES)—Finance Code 001. The authors also thank the support provided by the Civil Engineering Department (http://www.dec.ufv.br/), Nucleus of Microscopy and Microanalysis (https://nmm.ufv.br/) and Department of Physics (https://www.dpf.ufv.br/) of the Federal University of Viçosa.

Conflicts of Interest: The authors declare no conflicts of interest.

Abbreviations

The following abbreviations are used in this manuscript:

HMA	Hot Mix Asphalt
DNIT	Departamento Nacional de Infraestrutura de Transportes (Brazilian National Department of Transport Infrastructure)
ABNT	Associação Brasileira de Normas Técnicas (Brazilian Association of Technical Standards)
AV	Air Voids
VFA	Voids Filled with Asphalt
TS	Tensile Strength (By Diametral Compression)
RM	Resilient Modulus
RM/TS	Ratio between Resilient Modulus and Tensile Strength
Mc	Creep Modulus
Dt	Total Deformation
I-curve	Slope of the Secondary Phase of the Deformation Curve (From Static Creep Test)
Nf	Fatigue Life (Number of Load Cycles to Failure)
Nf,lab	Laboratory Fatigue Life
σh	Horizontal Stress
σv	Vertical Stress
Δσ	Stress Difference
ME	Método de Ensaio (Test Method, DNIT Standards)
NBR	Norma Brasileira (Brazilian Standard)
Q1, Q2, Q3	Axle Loads Applied in Elsym5 Analysis (80 kN, 98 kN, and 118 kN, respectively)
q1, q2, q3	Wheel loads
P1, P2, P3	Tire Inflation Pressures (563, 633, and 703 kPa, respectively)
Dadm	Allowable Recoverable Deflection
Elsym5	Elastic Layer System Model (Pavement Structural Analysis Software)
PRO	Procedimento (Procedure, DNER Standards)
DNER	Departamento Nacional de Estradas de Rodagem (Brazilian Highway Department)
REGAP	Refinaria Gabriel Passos (Brazilian Oil Refinery, Betim/MG)

References

1. Albayati, A.H.; Abduljabbar, M.H. The simulation of short-term aging based on the moisture susceptibility of asphalt concrete mixtures. *Results Eng.* **2019**, *2*, 100012. [CrossRef]
2. Liu, X.; Li, B.; Jia, M.; Li, C.; Zhang, Z. Effect of short-term aging on interface-cracking behaviors of warm mix asphalt under dry and wet conditions. *Constr. Build. Mater.* **2020**, *261*, 119885. [CrossRef]
3. Briliak, D.; Remišová, E. Research into effect of asphalt mixture aging on stiffness. *Transp. Res. Procedia* **2021**, *55*, 1251–1257. [CrossRef]
4. *ME 447*; Asphalt Mixtures—Marshall Stability and Creep Test—Test Method. DNIT: Brasília, Brazil, 2024; p. 9.

5. Shah, S.A.R.; Anwar, M.K.; Arshad, H.; Qurashi, M.A.; Nisar, A.; Khan, A.N.; Waseem, M. Marshall stability and flow analysis of asphalt concrete under progressive temperature conditions: An application of advance decision-making approach. *Constr. Build. Mater.* **2020**, *262*, 120756. [CrossRef]
6. Pradhan, S.K. Short-term and long-term aging effect of the rejuvenation on RAP binder and mixes for sustainable pavement construction. *Int. J. Transp. Sci. Technol.* **2023**, *12*, 937–954. [CrossRef]
7. Li, R.; Li, X.; Yue, J.; Yang, C. Effects of salt solution-aging coupling on viscoelastic, fatigue and self-healing properties of asphalt binder. *Constr. Build. Mater.* **2024**, *419*, 135514. [CrossRef]
8. Mohammad Asib, A.S.; Rahman, R.; Romero, P.; Hoepfner, M.P.; Mamun, A. Physicochemical characterization of short and long-term aged asphalt mixtures for low-temperature performance. *Constr. Build. Mater.* **2022**, *319*, 126038. [CrossRef]
9. Zheng, Q.; He, P.; Zhang, D.; Weng, Y.; Lu, J.; Wang, T. A Holistic View of Asphalt Binder Aging under Ultraviolet Conditions: Chemical, Structural, and Rheological Characterization. *Buildings* **2024**, *14*, 3276. [CrossRef]
10. Sun, S.; Li, P.; Su, J.; Ma, Y.; Wang, X.; Bi, J. Study on deformation behavior and prediction model of asphalt mixture based on interface-slip characteristics of aggregates. *Constr. Build. Mater.* **2021**, *294*, 123581. [CrossRef]
11. Tejeshwini, S.; Gowda, C.M.P.; Mamatha, K.H.; Balreddy, M.S.; Dinesh, S.V. Impact of antiaging additives on the conventional properties of bituminous binder. *J. Eng. Appl. Sci.* **2024**, *71*, 184. [CrossRef]
12. da Silva, T.O.; Pitanga, H.N.; Silva, N.A.B.; Cardoso, H.S.; Lopes, E.C.; Rodrigues, K.H.d.P.; Nalon, G.H.; Borges, P.R. Effects of short-term aging on the mechanical and structural performance of hot mix asphalt mixtures: A case study complemented by statistical analysis. *Road Mater. Pavement Des.* **2025**, *26*, 203–216. [CrossRef]
13. Nie, F.; Su, X.; Wang, M.; Ma, X.; Ou, K.; Liu, J.; Lin, H. Debonding of asphalt-aggregate interface under coupled moisture and temperature conditions: An atomistic study. *Case Stud. Constr. Mater.* **2025**, *22*, e04554. [CrossRef]
14. Wu, X.; Chen, C.; Zheng, Y.; Chen, S.; Luo, H.; Chen, S.; Huang, X.; Ma, T. Impact of aggregate types, dosages, and binder levels on pavement early bonding and skid resistance: An enhanced laboratory wear analysis. *Case Stud. Constr. Mater.* **2025**, *22*, e04584. [CrossRef]
15. *NBR 17054*; Agregados—Determinação da Composição Granulométrica. ABNT: São Paulo, Brazil, 2022.
16. *NBR 16973*; Agregados—Determinação do Material Fino que Passa Pela Peneira de 75 mm por lava Gem. ABNT: São Paulo, Brazil, 2021.
17. *ME 424*; Pavimentação—Agregado—Determinação do Índice de Forma Com Crivos. DNIT: Brasília, Brazil, 2020.
18. *NBR 6458*; Grãos de Pedregulho Retidos na Peneira de Abertura 4.8 mm—Determinação da Massa Específica, da Massa Específica Aparente e da Absorção de Água. ABNT: São Paulo, Brazil, 2017.
19. *NBR 16974*; Agregados—Ensaio de Resistência ao Impacto e à Abrasão Los Angeles. ABNT: São Paulo, Brazil, 2022.
20. *NBR 12583*; Agregado Graúdo—Determinação da Adesividade ao Ligante Betuminoso. ABNT: São Paulo, Brazil, 2017.
21. *NBR 6576*; Materiais Asfálticos—Determinação da Penetração. ABNT: São Paulo, Brazil, 2007.
22. *NBR 6560*; Ligantes Asfálticos—Determinação do Ponto de Amolecimento. ABNT: São Paulo, Brazil, 2016.
23. *NBR 11341*; Derivados do Petróleo—Determinação dos Pontos de Fulgor e de Combustão em Vaso Aberto Cleveland. ABNT: São Paulo, Brazil, 2015.
24. *NBR 6296*; Produtos Betuminosos Semissólidos—Determinação da Massa Específica e Densidade Relativa. ABNT: São Paulo, Brazil, 2013.
25. *NBR 6293*; Ligantes Asfálticos—Determinação da Ductilidade. ABNT: São Paulo, Brazil, 2015.
26. *NBR 15235*; Materiais Asfálticos—Determinação do Efeito do Calor e do ar em uma Película Delgada Rotacional. ABNT: São Paulo, Brazil, 2009.
27. *NBR 14855*; Ligantes Asfálticos—Determinação da Solubilidade em Tricloroetileno. ABNT: São Paulo, Brazil, 2015.
28. *NBR 15184*; Materiais Betuminosos—Determinação da Viscosidade em Temperaturas Elevadas Usando um Viscosímetro Rotacional. ABNT: São Paulo, Brazil, 2021.
29. DNIT. *Manual de Pavimentação*; DNIT: Rio de Janeiro, Brazil, 2006; p. 274.
30. *ME 004*; Bituminous Material—Determination of Saybolt-Furol Viscosity at High Temperature by Thin Film Method. DNER: Rio de Janeiro, Brazil, 1994; p. 2.
31. Bernucci, L.B.; Motta, L.d.; Ceratti, J.A.P.; Soares, J.B. *Pavimentação Asfáltica: Formação Básica Para Engenheiros*, 2nd ed.; ABEDA: Rio de Janeiro, Brazil, 2022; p. 750.
32. *ME 136*; Asphalt Paving—Asphalt Mixtures—Determination of Tensile Strength by Diametrical Compression—Test Method. DNIT: Rio de Janeiro, Brazil, 2018; p. 9.
33. *ME 135*; Asphalt Paving—Asphalt Mixtures—Determination of the Resilient Modulus—Test Method. DNIT: Rio de Janeiro, Brazil, 2018; p. 13.
34. *ME 183*; Asphalt Paving—Controlled Stress Diametrical Compression Fatigue Test—Test Method. DNIT: Rio de Janeiro, Brazil, 2018; p. 15.

35. National Cooperative Highway Research Program. *Simple Performance Test for Superpave Mix Design*; 0309-2755; Transportation Research Board, National Research Council: Washington, DC, USA, 2002.
36. Ponte, R.S.; Castelo Branco, V.T.F.; de Holanda, Á.S.; Soares, J.B. Avaliação de diferentes metodologias para obtenção do Módulo de Resiliência de misturas asfálticas. *Transportes* **2014**, *22*, 85–94. [CrossRef]
37. *ME 133*; Asphalt Paving—Delineation of the Longitudinal Influence Line of the Deformation Basin Using the Benkelman Beam—Test Method. DNIT: Rio de Janeiro, Brazil, 2010; p. 8.
38. Carmo, C.; Silva, T.; Marques, G.; Pereira, G.S.; Pitanga, H.N. Avaliação do comportamento mecânico de misturas asfálticas dosadas pelo método MARSHALL reforçadas com geogrelha. In Proceedings of the VIII Congresso Brasileiro de Geossintéticos, São Carlos, Brazil, 14–16 August 2019.
39. Yang, X.; Peng, C.; Chen, J.; Liu, G.; He, X. Effect of short-term aging on rheological properties of bio-asphalt/SBS/PPA composite modified asphalt. *Case Stud. Constr. Mater.* **2023**, *19*, e02439. [CrossRef]
40. Li, B.; Zhou, J.; Zhang, Z.; Yang, X.; Wu, Y. Effect of Short-Term Aging on Asphalt Modified Using Microwave Activation Crumb Rubber. *Materials* **2019**, *12*, 1039. [CrossRef]
41. dos Santos, K.P.; Lucena, A.E.d.F.L.; Lucena, L.C.d.F.L.; e Silva, J.d.A.A.; Costa, S.C.F.d.E. Estudo da incorporação de argilas montmorilonitas em cimentos asfálticos de petróleo. *Matéria* **2015**, *20*, 501–513. [CrossRef]
42. Campelo, N.; Silva, F.; Andrade, J. Use of Wastewater Treatment Sludge (WTS) as Filler in Hot-Mixed Asphalt Concrete. *Int. J. Waste Resour.* **2020**, *10*, 379. [CrossRef]
43. Babadopulos, L.F.d.A.L.; Ferreira, J.L.S.; Soares, J.B. An approach to couple aging to stiffness and permanent deformation modeling of asphalt mixtures. *Mater. Struct.* **2016**, *49*, 4929–4945. [CrossRef]
44. Little, D.N.; Button, J.W.; Youssef, H. *Development of Criteria to Evaluate Uniaxial Creep Data and Asphalt Concrete Permanent Deformation Potential*; Texas Transportation Institute, Texas A&M University, TTL/CE Building: College Station, TX, USA, 1993.
45. Ziari, H.; Saghafi, Y.; Moniri, A.; Bahri, P. The effect of polyolefin-aramid fibers on performance of hot mix asphalt. *Pet. Sci. Technol.* **2020**, *38*, 170–176. [CrossRef]
46. DNER. *PRO 11—Avaliação Estrutural de Pavimentos Flexíveis*; Rio de Janeiro, Brazil, 1979; p. 16.
47. Wu, M.; Yin, L.; Li, M.; You, Z.; Jin, D.; Xin, K. A state-of-the-art review of asphalt aging behavior at macro, micro, and molecular scales. *Constr. Build. Mater.* **2025**, *460*, 139738. [CrossRef]
48. Ahmad, M.; Khedmati, M.; Mensching, D.; Hofko, B.; Haghshenas, H.F. Aging characterization of asphalt binders through multi-aspect analyses: A critical review. *Fuel* **2024**, *376*, 132679. [CrossRef]
49. Hu, Y.; Si, W.; Kang, X.; Xue, Y.; Wang, H.; Parry, T.; Airey, G.D. State of the art: Multiscale evaluation of bitumen ageing behaviour. *Fuel* **2022**, *326*, 125045. [CrossRef]

Disclaimer/Publisher's Note: The statements, opinions and data contained in all publications are solely those of the individual author(s) and contributor(s) and not of MDPI and/or the editor(s). MDPI and/or the editor(s) disclaim responsibility for any injury to people or property resulting from any ideas, methods, instructions or products referred to in the content.